

Wigner crystals for a planar, equimolar binary mixture of classical, charged particles

Moritz Antlanger^{1,2, a)} and Gerhard Kahl¹

¹⁾*Institut für Theoretische Physik and Center for Computational Material Science (CMS), Vienna University of Technology, AUSTRIA*

²⁾*Laboratoire de Physique Théorique (UMR 8627), Université de Paris-Sud and CNRS, Bâtiment 210, 91405 Orsay Cedex, FRANCE*

We have investigated the ground state configurations of an equimolar, binary mixture of classical charged particles (with nominal charges Q_1 and Q_2) that condensate on a neutralizing plane. Using efficient Ewald summation techniques for the calculation of the ground state energies, we have identified the energetically most favourable ordered particle arrangements with the help of a highly reliable optimization tool based on ideas of evolutionary algorithms. Over a large range of charge ratios, $q = Q_2/Q_1$, we identify six non-trivial ground states, some of which show a remarkable and unexpected structural complexity. For $0.59 \lesssim q < 1$ the system undergoes a phase separation where the two charge species populate in a hexagonal arrangement spatially separated areas.

PACS numbers: 52.27.Lw, 64.70.K-, 64.75.St, 73.20.Qt

Keywords: Wigner crystals, binary mixture of charged systems, ground states, Ewald summation, evolutionary algorithm

^{a)}moritz.antlanger@tuwien.ac.at

I. INTRODUCTION

The identification of the ordered ground state configurations of classical charged particles is known in literature as the Wigner problem¹. In two dimensions and at vanishing temperature these charges form a hexagonal lattice²⁻⁴. In rather recent investigations, this problem has been extended: one example is the bilayer problem where the charges are confined between two planes, which are separated by a finite distance^{5,6}. Due to the availability of closed, analytic expressions for the potential energy of this particular system, the complete set of its ground state configurations could be identified.

In the present contribution we return to the single layer problem and consider an equimolar, binary mixture of charged particles (with nominal values Q_1 and Q_2), that condensate at vanishing temperature on a neutralizing plane. For given values Q_1 and Q_2 the ordered equilibrium configurations of the particles at vanishing temperature are imposed by the requirement that the potential energy is minimized. With the help of efficient and highly accurate Ewald summation techniques⁷, the lattice sum of this system can be evaluated for any particle arrangement on an arbitrary, two-dimensional lattice. Employing suitable optimization techniques, the parameters of these lattices are then optimized in such a way as to minimize the lattice sum. In this contribution we have used an optimization tool that is based on ideas of evolutionary algorithms (EAs)^{8,9}. Within this concept, any possible two-dimensional lattice is considered as an individual, to which a fitness value is assigned. These individuals are then exposed on the computer to an artificial evolution: via creation and mutation operations a large number of individuals is produced; in the former procedure a pair of new individuals is created from a pair of parent individuals which are selected according to their fitness values. Along this evolution only the best, *i.e.*, the fittest, individuals are expected to survive and are thus retained. Bearing in mind that we are looking for the individual (= structure) with the lowest lattice sum, we assign a high fitness value to an energetically favourable ordered structure. EA-based optimization algorithms have turned out to be highly efficient and reliable tools for identifying ordered equilibrium structures in a broad variety of condensed matter systems, in general⁹⁻¹², and for quite a few two-dimensional systems, in particular¹³⁻¹⁷.

In total we have identified six non-trivial ground states. They are characterized by a broad variety of structural complexity, which is the result of an intricate competition

between the interactions of the two charges. Introducing the charge ratio q as the only relevant parameter of the system (defined as $q = Q_2/Q_1$ with $0 \leq q \leq 1$ due to simple consideration and due to symmetry arguments) we identified two structures that show a remarkable stability over relatively large q -ranges: (i) one of them can be described via two intertwining, commensurate square sublattices, one of them populated by charges Q_1 , the other by charges Q_2 ; this structure shows, in addition, among all ground states the highest energy gain with respect to a suitably defined reference state; (ii) in the other ordered equilibrium configuration strongly distorted, but symmetric hexagonal tiles cover the entire two-dimensional space hosting in their interiors pairs of the weaker charges. For $0.59 \lesssim q < 1$ the system undergoes a phase separation where the two spatially separated phases are represented by hexagonal lattices populated by either species of charges. The remaining four non-trivial ground states are dominated by distorted, asymmetric hexagonal arrangements of charges Q_1 , hosting in their interior pairs and triplets of charges Q_2 . For the limiting values, *i.e.*, $q = 0$ and $q = 1$, we obtain the expected hexagonal particle arrangements.

The paper is organized as follows. In the subsequent section we briefly introduce our model system. Section 3 is dedicated to the methods we have used: both the Ewald summation technique as well as our optimization tool (based on ideas of evolutionary algorithms) are briefly summarized; further we introduce a suitable state of reference for our energetic considerations. In section 4 we thoroughly discuss the results. The contribution is closed with concluding remarks.

II. MODEL

We consider an equimolar mixture of classical charges with the particles being confined to a planar (*i.e.*, two-dimensional) geometry. The point charges (with nominal values Q_1 and Q_2) are located at positions \mathbf{r}_i and \mathbf{r}_j and interact via an unscreened Coulomb interaction

$$\Phi(r_{ij}) = \frac{Q_i Q_j}{r_{ij}} \quad (1)$$

with $r_{ij} = |\mathbf{r}_i - \mathbf{r}_j|$.

Since the total number density (*i.e.*, number of particles per unit area), ρ , can be scaled out via the distances, its actual quantity is irrelevant for further considerations. In the

equimolar case we obtain for the partial number densities $\rho_1 = \rho_2 = \rho/2$.

For convenience we introduce the parameter $q = Q_2/Q_1$, *i.e.*, the ratio between the two types of charges. Since negative values of q lead to a divergent potential energy and taking into account the symmetry $q \leftrightarrow 1/q$ we can restrict ourselves to the range $0 \leq q \leq 1$; thus we assume that charge Q_1 is stronger than charge Q_2 . Note that we recover the classical Wigner problem for $q = 1$.

To compensate for the charges, we introduce a uniform, neutralizing background on the plane, specified by a charge density σ , which is given by

$$\sigma = -\rho_1 Q_1 - \rho_2 Q_2 = -Q_1 \frac{1+q}{2} \rho. \quad (2)$$

III. METHOD

The present contribution is dedicated to a complete identification of the ground state configurations of an equimolar mixture of point charges, *i.e.*, the ordered equilibrium structures at vanishing temperature. Following the basic laws of thermodynamics, the particles will arrange under these conditions in an effort to minimize the corresponding thermodynamic potential. For our system (*i.e.*, fixed particle number N and density ρ), we have to minimize the potential energy, which reduces at vanishing temperature to the lattice sum of the ordered particle configuration.

Among the numerous optimization schemes available in literature, we have opted for an optimization algorithm that is based on ideas of EAs^{8,9}. Our choice is motivated by the fact that this strategy has turned out to be highly successful in related problems for a wide variety of soft matter systems, including in particular problems in two-dimensional geometries¹³⁻¹⁷. For a comprehensive presentation of this optimization algorithm and of the related computational and numerical details, we refer the reader to^{9,18}.

The quantity that has to be minimized is the lattice sum of an ordered particle configuration. Taking into account the long-range character of the interactions (1), this quantity can most conveniently be calculated via Ewald sums⁷. For the separation of r - and k -space contributions, we have used the cutoff values $r_c = 15/\sqrt{\rho}$ and $k_c = 10\sqrt{\rho}$, respectively; for the Ewald summation parameter we use $\alpha = 0.3$. This set of numerical parameters guarantees a relative accuracy of 10^{-5} for the evaluation of the internal energy.

In an effort to specify the ordered structures, we introduce for convenience a q -dependent reference energy. For the one component system (*i.e.*, $q = 1$) the ground state energy (per particle) of point charges, arranged on a neutralizing plate in a hexagonal lattice, is given by ($Q = Q_1 = Q_2$)

$$E_0(q = 1) = -C_M \sqrt{\rho} Q^2, \quad (3)$$

$C_M = 1.960515789$ being the Madelung constant of this particular particle arrangement.

We extend this expression continuously to $q \leq 1$ along the following lines: we imagine the system to be split up into two infinitely large regions, labeled $\gamma = 1$ and $\gamma = 2$, each of them hosting exclusively the respective charges, Q_1 and Q_2 , and each of them being locally charge neutral. The two regions share a common border. Introducing local number densities, $\rho_i^{(\gamma)}$, for species i in region γ ($i = 1, 2$ and $\gamma = 1, 2$), we arrive at the following relations:

$$\begin{aligned} \rho_1^{(1)} Q_1 + \sigma &= 0 & \rho_2^{(1)} &= 0 \text{ in region 1} \\ \rho_1^{(2)} &= 0 & \rho_2^{(2)} Q_2 + \sigma &= 0 \text{ in region 2.} \end{aligned}$$

Together with (2), we obtain

$$\rho_1^{(1)} = \frac{1+q}{2} \rho \quad \text{in region 1} \quad \rho_2^{(2)} = \frac{1+q}{2q} \rho \quad \text{in region 2.} \quad (4)$$

With these values for the local number densities and assuming that the charges will form hexagonal lattices in the respective regions, we obtain – with the help of equation (3) – the total energy per particle for this system

$$\begin{aligned} E_0(q) &= -C_M \left(\frac{1}{2} \sqrt{\rho_1^{(1)}} Q_1^2 + \frac{1}{2} \sqrt{\rho_2^{(2)}} Q_2^2 \right) \\ &= -C_M \sqrt{\rho} Q^2 \sqrt{\frac{1+q}{2} \frac{1+q^{3/2}}{2}}. \end{aligned} \quad (5)$$

In an effort to characterize the emerging ground state configurations, we have evaluated the two-dimensional orientational bond order parameters, Ψ_4 and Ψ_6 ¹⁹, defined via

$$\Psi_n = \left| \frac{1}{N_i} \sum_{j=1}^{N_i} \exp[in\Theta_j] \right| \quad n = 4, 6. \quad (6)$$

N_i is the number of nearest neighbours of a tagged particle with index i and Θ_j is the angle of the vector connecting this particle with particle j with respect to an arbitrary, but fixed orientation.

IV. RESULTS

In an effort to identify the complete set of ordered ground state configurations of our system specified in Section II, we have performed extensive EA-runs, taking into account up to 20 particles per species and per unit cell. For a given state point, up to 5,000 individuals were created. Calculations have been performed on a discrete q -grid with a spacing of $\Delta q = 0.01$; thus in this contribution Δq defines the accuracy in the location of the boundaries between ground states. The respective minimum energy configurations were retained as the ground state particle arrangements.

In Figure 1 we display the energy (per particle), $E(q)$, of these ground state configurations and the energy difference, $\Delta E(q) = [E(q) - E_0(q)]$, with respect to the reference energy, $E_0(q)$, as defined in equation (5). Note that over the entire q -range $\Delta E(q)$ is very small, *i.e.*, less than 5×10^{-3} . The fact that the differences between competing structures are so small is a fingerprint of the long-range nature of the Coulomb interaction.

$E(q)$ decays with increasing q : it connects the limiting value at $q = 0$ [$E(q = 0) = E_0(q = 0) = -C_M \sqrt{\rho} Q^2 / 2\sqrt{2}$], obtained for a pure system of charges Q_1 and a number density $\rho_1 = \rho/2$ with the other reference state at $q = 1$, where the charges are indistinguishable (*i.e.*, $Q_1 = Q_2 = Q$) and thus $E(q = 1) = E_0(q = 1) = -C_M \sqrt{\rho} Q^2$. In the intermediate q -range, the curve seems – at first sight – to be a smooth, monotonous function. The subtle details, which reflect the structural changes of the system as q varies, become visible only if we subtract from $E(q)$ the reference energy, $E_0(q)$, *i.e.*, $\Delta E(q) = E(q) - E_0(q)$. This function is now non-monotonous and shows kinks for particular q -values which can be associated with the structural changes. For convenience, the vertical broken lines in Figure 1 indicate the limits of stability of the six non-trivial identified ground states. The fact that these kinks are sometimes more or less pronounced is related to three issues: (i) the limited accuracy of our energy evaluation (see discussion above), (ii) the finite grid-size Δq underlying our investigations, and (iii) the intersection angle between the $E(q)$ -curves of two neighbouring ground state structures. For $0.59 \lesssim q < 1$ the energy of the (phase separated)

TABLE I. Overview over the identified ground state configurations and the respective q -ranges. The structures themselves are depicted in Figures 2 – 5.

q -range	ground state structure
0.00	hexagonal lattice formed by charges Q_1
$0.00 < q \lesssim 0.04$	Structure 1
$0.05 \lesssim q \lesssim 0.09$	Structure 2
$0.10 \lesssim q \lesssim 0.25$	Structure 3
$0.26 \simeq q$	Structure 4
$0.27 \lesssim q \lesssim 0.28$	Structure 5
$0.29 \lesssim q \lesssim 0.59$	Structure 6
$0.60 \lesssim q < 1$	phase separation
1.00	hexagonal lattice formed by the (indistinguishable) charges Q_1 and Q_2

reference state, $E_0(q)$, attains values that are smaller than the energy of the respective ground states identified in our EA search, indicating that the system undergoes a phase separation. This phenomenon, *i.e.*, the formation of two *infinitely* large regions populated by only one species of charges representing the coexisting phases, cannot be grasped with our EA-based optimization tool, since it relies on a *finite* number of charges per unit cell.

The Table provides an overview over the ground state configurations that we have identified for $0 \leq q \leq 1$; the structures themselves are depicted in Figures 2 – 5.

For $\mathbf{q} = \mathbf{0}$, charges with non-vanishing nominal values, Q_1 , arrange – as expected – in a hexagonal lattice (not depicted) with number density $\rho_1 = \rho/2$; the other, chargeless particles do not interact with any particle species and thus occupy arbitrary positions.

For $\mathbf{0} < \mathbf{q} \lesssim \mathbf{0.04}$, charges Q_1 form a hexagonal lattice which is to a high degree regular (Structure 1, depicted in the left panel of Figure 2): the order parameter Ψ_6 varies between $\Psi_6(q = 0.01) = 0.99972$ and $\Psi_6(q = 0.04) = 0.99577$. The deviation from its ideal value, $\Psi_6 = 1$, stems from a slight distortion of these hexagons (highlighted in the corresponding panel): a central 'axis' (dotted line in the corresponding panel), connecting the 'upper' and 'lower' vertices of the hexagon, is formed by two line-segments of equal length; the distances

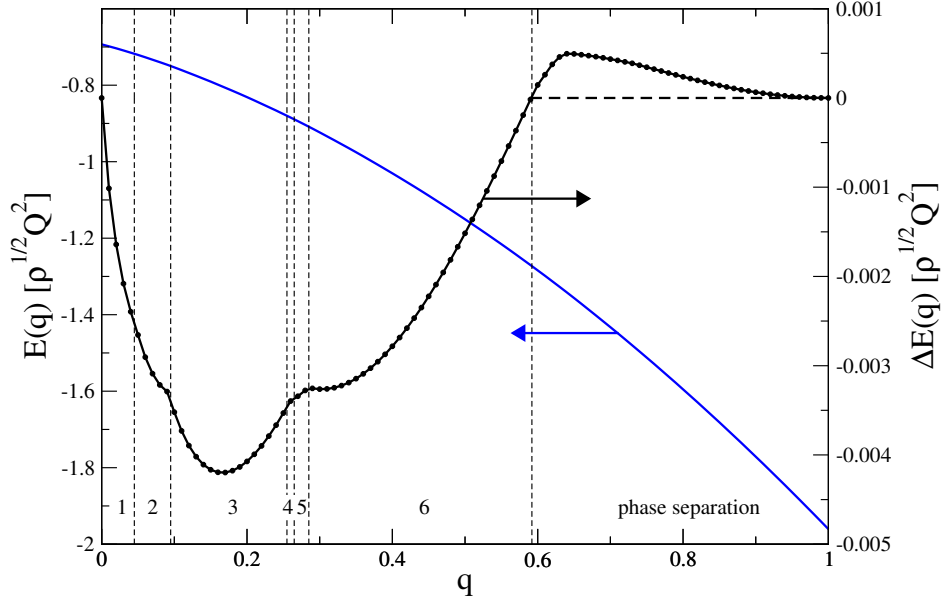


FIG. 1. Energy per particle of the ground state configuration, $E(q)$ (blue line), and energy difference (per particle), $\Delta E(q) = [E(q) - E_0(q)]$ (black line), with respect to the reference energy, $E_0(q)$, as defined in equation (5) as functions of q . Vertical broken lines indicate the limits of stability of the six identified non-trivial ground states. The horizontal broken line marks the q -values where the phase separated system is the energetically most favourable one.

of the vertices left (right) to this central axis from the center of the hexagon differ in their length by less than +4% (-3 %). Thus the left half of the hexagon is slightly larger than its counterpart located to the right of the central axis. This enlarged space is imposed by the fact that this area hosts charges Q_2 , which form a zig-zag pattern within the ground state configuration, oriented parallel to the central axis of the hexagon; within this line, charges Q_2 are equidistant. The other part of the hexagon, located right to its central axis remains empty.

In the adjacent q -range, $0.05 \lesssim q \lesssim 0.09$, charges Q_1 maintain their hexagonal arrangements (Structure 2, displayed in the right panel of Figure 2). As compared to Structure 1, the distortion of the hexagons (highlighted in the corresponding panel) is now considerably more pronounced: $\Psi_6(q = 0.05) = 0.90598$ while $\Psi_6(q = 0.09) = 0.83643$. The 'upper' and the 'lower' vertices of the hexagon are still connected via a central axis (dotted line in the corresponding panel), consisting of two line segments of equal length; however, the distances of the vertices left to this central axis from the center of the hexagon are now by up to 21 % longer, while the corresponding distances of the vertices on the opposite side of the

axis are less than 5 % shorter. This conceivable asymmetry (see the highlighted hexagon in the corresponding panel) is imposed by the increased nominal value of charge Q_2 : the zig-zag arrangement of particles, observed for this species of charges in Structure 1 has been replaced by a parallel arrangements of pairs of particles which are aligned in the direction of the central axis of the hexagon; while the intra-pair distance is very short, the inter-pair distance is quite large.

In the relatively wide range of $0.10 \lesssim q \lesssim 0.25$ the two species of charges arrange in two intertwining, commensurate square lattices (Structure 3, cf. Figure 3). It has to be emphasized that both sublattices remain perfect over the entire q -range of stability, *i.e.*, $\Psi_4 = 1$ for $0.10 \lesssim q \lesssim 0.25$. The structural stability of this particular ground state is also reflected by the fact that Structure 3 is characterized by the highest energy gain compared to the energy value of the reference structure, $E_0(q)$ (see Figure 1).

Around the value $q \simeq 0.26$, charges Q_1 form hexagonal structural units which are in their shape reminiscent of gems or diamonds. These six-particle rings form in a head-to-tail arrangement *parallel* lanes: adjacent six-particle rings of neighbouring lanes share vertices, while the remaining edges form equilateral triangles. This ground state is referred to as Structure 4; it is depicted in the left panel of Figure 4 and the six-particle rings are highlighted. Each of the six-particle units hosts in its center an essentially equilateral triangle of charges Q_2 . The positions of the six surrounding charges Q_1 are imposed by the condition that the smallest distance of these charges from any of the three inner charges (Q_2) has the same value; this requirement induces the particular shape of the six-particle rings. The triangular arrangements that fill up the interstitial space are not populated by charges Q_2 .

The ground state identified for $0.27 \lesssim q \lesssim 0.28$ (denoted as Structure 5 and depicted in the right panel of Figure 4) differs only in one feature from Structure 4: the lanes, formed by the head-to-tail arrangements of the six-particle rings (highlighted in the corresponding panel) are now *antiparallel*. In this configuration the neighbouring rings of adjacent lanes share edges, which leads now to the formation of rhombic four-particle arrangements which are again void of Q_2 charges.

Finally, at $q \simeq 0.29$ Structure 6 emerges and remains the ground state over the relatively large interval $0.29 \lesssim q \lesssim 0.59$ (see left panel of Figure 5). Its basic unit is an elongated hexagon (highlighted in the corresponding panel): aligned in parallel and sharing edges with

neighbouring tiles, they completely cover the two-dimensional space. The direction perpendicular to the longest elongation of this hexagon is considered for the following discussion as the central axis (dotted in the corresponding panel). For Structure 6 this axis is also the symmetry axis of the hexagon. The four edges originating from the central axis have the same lengths, say l_1 ; similarly, the remaining two edges of the hexagon (oriented parallel to the central axis) assume another, equal value, say l_2 . Each of these hexagons hosts a pair of charges Q_2 , located on a line perpendicular to the central axis and separated by a distance, which decreases as q is increased. By increasing the charge ratio q , l_1 decreases from $1.297\sqrt{\rho}$ (at $q = 0.29$) to $1.269\sqrt{\rho}$ (at $q = 0.59$), while l_2 increases from $1.29\sqrt{\rho}$ (at $q = 0.29$) to $1.324\sqrt{\rho}$ (at $q = 0.59$). At the cross-over, *i.e.*, $l_1 \simeq l_2$ (observed for $q \simeq 0.36$, our optimization tool identifies a closely related, energetically degenerate structure, denoted as Structure 6' and depicted in the right panel of Figure 5: now that all edges of the basic hexagon are equal, these units are no longer forced to align in parallel, but are able to chose an alternative, non-parallel arrangement: imposed by the internal angle between edges of the basic hexagon, these units arrange in a grain-like super-structure.

For $0.59 \lesssim q < 1.00$, we find that $E_0(q) < E(q)$ (see Figure 1), indicating that the phase separated particle configuration is energetically more stable than any other ordered structure identified by our optimization tool. Due to the limitation in the number of particles per unit cell, the EA-based search for ground state configurations proposes – depending on the number of particles per cell – configurations with increasing complexity, all of them being characterized by an energy value $E(q)$ that is larger than the corresponding value $E_0(q)$. Thus the demixed state, formed by two separate hexagonal, ordered regions and each of them being populated by one species of charge, is the ground state in this q -range.

Finally, for $q = 1$, we recover the one-component hexagonal monolayer (not displayed).

V. CONCLUSIONS

In this contribution we have investigated the ground state configurations of an equimolar, binary mixture of classical charged particles (with nominal charges Q_1 and Q_2), that self-assemble on a neutralizing plane. Our investigations are based on reliable Ewald summation techniques which allow an efficient evaluation of the ground state energies (= lattice sums). With the help of reliable optimization tools, which are based on ideas of evolu-

tionary algorithms, we are able to identify the ordered ground states of the system: by searching essentially among all possible two-dimensional lattices, this algorithm identifies for a given charge ratio $q = Q_2/Q_1$ the energetically most favourable particle arrangement. Apart from the expected, trivial hexagonal lattices for $q = 0$ and $q = 1$, we could identify for $0 < q \lesssim 0.59$ in total six ground state configurations.

Quite unexpectedly, these particle arrangements show a remarkable structural complexity which is the result of the energetic competition between the charge-charge interactions. Throughout, a pronounced impact of the weaker charges, Q_2 , on the sublattices formed by the stronger charges, Q_1 , could be observed: this holds even if the corresponding q -values are rather small (*i.e.*, $q \simeq 0.05$). Except for a purely square particle arrangement (which is stable over a remarkably large q -range and which shows the highest energy gain among all ground states with respect to a suitably defined reference state – see also the discussion about energies below), the ground states can be described on the basis of asymmetric, sometimes strongly distorted six-particle arrangements formed by charges Q_1 , which host in their interior simple two- or three-particle configurations of charges Q_2 . A deeper insight into the mechanisms that govern the formation of ground states is gained by introducing a phase separated reference state, where the two species of charges populate in hexagonal arrangements spatially separated areas. Comparing the energies of our ground state configurations, $E(q)$, with the energy of this reference state, $E_0(q)$, we find that these two functions differ by less than 5×10^{-3} , a fact that represents a characteristic fingerprint of the long-range Coulomb interactions. An analysis of this energy difference as a function of q reveals that transitions from one ground state to an adjacent one become visible as (more or less pronounced) kinks in this function. Based on these considerations we could show that for $0.59 \lesssim q < 1$ the energetically most favourable particle arrangement is the (ideal) phase separated state.

ACKNOWLEDGMENTS

This work was financially supported by the Austrian Research Fund (FWF) under Proj. No. P23910-N16. The authors gratefully acknowledge discussions with Martial Mazars (Paris-Orsay), Ladislav Šamaj (Bratislava), and Emmanuel Trizac (Paris-Orsay).

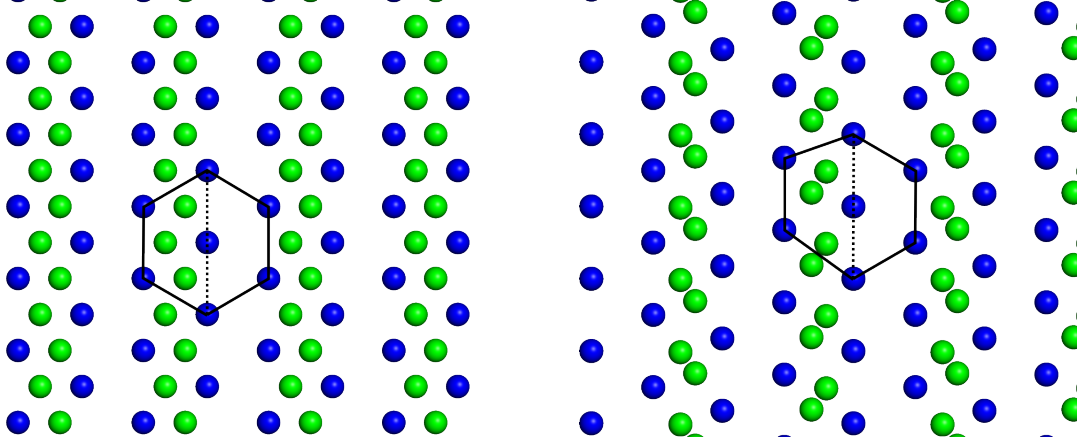


FIG. 2. Left panel: structure 1 (identified for $q = 0.02$), right panel: structure 2 (identified for $q = 0.05$). Blue: charges Q_1 , green: charges Q_2 . Lines highlight the hexagonal units discussed in the text. The dotted lines mark the central axes of the hexagonal units (cf. text).

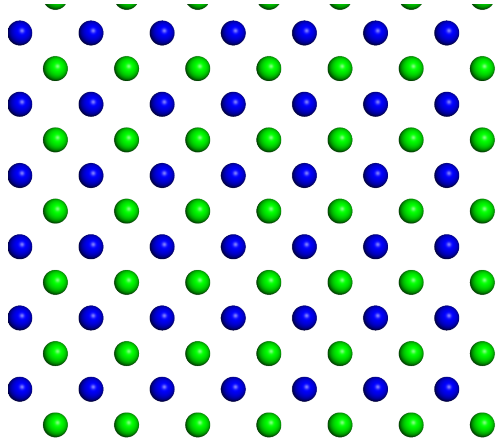


FIG. 3. Structure 3 (identified for $q = 0.10$). Blue: charges Q_1 , green: charges Q_2 .

REFERENCES

- ¹Wigner E., Phys. Rev., 1934, **46**, 1002.
- ²Meißner G., Namaizawa H., Voss M., Phys. Rev. B, 1976, **13**, 1370.
- ³Bonsall L., Maradudin A. A., Phys. Rev. B, 1977, **15**, 1959.
- ⁴Levin Y., Rep. Prog. Phys., 2002, **65**, 1577.
- ⁵Šamaj L., Trizac E., EPL, 2012, **98**, 36004.
- ⁶Šamaj L., Trizac E., Phys. Rev. B, 2012, **85**, 20513.

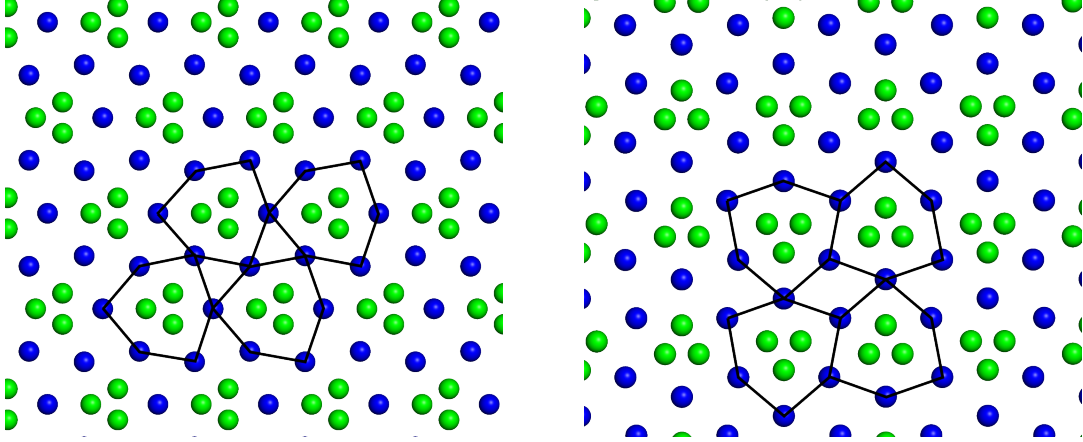


FIG. 4. Left panel: structure 4 (identified for $q = 0.26$), right panel: structure 5 (identified for $q = 0.27$). Blue: charges Q_1 , green: charges Q_2 . Lines highlight the hexagonal units discussed in the text.

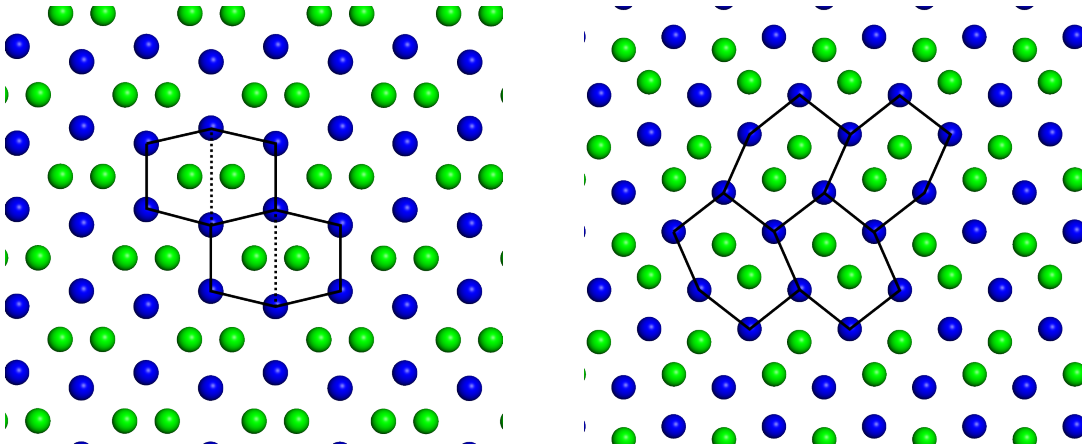


FIG. 5. Left panel: structure 6 (identified for $q = 0.30$), right panel: structure 6' (identified for $q = 0.35$). Blue: charges Q_1 , green: charges Q_2 . Lines highlight the hexagonal units discussed in the text. The dotted lines mark the central axes of the hexagonal units (cf. text).

⁷Mazars M., Phys. Rep., 2011, **500**, 43.

⁸Adaptation in Natural and Artificial Systems. Holland J. H., The University of Michigan Press, Ann Arbor, 1975.

⁹Gottwald D., Kahl G., Likos C., J. Chem. Phys., 2005, **122**, 204503.

¹⁰Pauschenwein G.J., Kahl G., J. Chem. Phys., 2008, **129**, 174107.

¹¹Kahn M., Weis J.J., Likos C.N., Kahl G., Soft Matter, 2009, **5**, 2852.

- ¹²Kahn M., Weis J.J., Kahl G., J. Chem. Phys., 2010, **133**, 224504.
- ¹³Fornleitner J., Kahl G., EPL, 2008, **82**, 18001.
- ¹⁴Fornleitner J., Lo Verso F., Kahl G., Likos C.N., Soft Matter, 2008, **4**, 480.
- ¹⁵Fornleitner J., Lo Verso F., Kahl G., Likos C., Langmuir, 2009, **25**, 7836.
- ¹⁶Doppelbauer G., Bianchi E., Kahl G., J. Phys.: Condens. Matter, 2010, **22**, 10410.
- ¹⁷Antlanger M., Doppelbauer G., Kahl G., J. Phys.: Condens. Matter, 2011, **23**, 404206.
- ¹⁸Doppelbauer G., Noya E.G., Bianchi E., Kahl G., Soft Matter, 2012, **8**, 7768.
- ¹⁹Strandburg K.J., Rev. Mod. Phys., 1988, **60**, 161.